STABILITY AND CHAOS IN PASSIVE-DYNAMIC LOCOMOTION

M.J. COLEMAN, M. GARCIA, A. L. RUINA AND J. S. CAMP
Department of Theoretical and Applied Mechanics
Cornell University, Ithaca, NY 14853-7501

AND

A. CHATTERJEE
Engineering Science and Mechanics
Penn State University, University Park, PA 16802

1. Introduction

Human locomotion is a complicated process, controlled and actuated by the neuro-muscular system. Tad McGeer [8], however, studied bipedal walking and completely neglected the neuro-muscular system in his models. Some of his machines, powered only by gravity, can walk stably and somewhat anthropomorphically down shallow slopes. We have continued study of the dynamics of McGeer-like physical and mathematical biped models that have little or no actuation or control. This paper summarizes some of our results.

These passive-dynamic walking mechanisms are built of hinged bodies that make collisional and rolling contact with the ground at the foot. In models with knees, the lower leg, or shank, is prevented from hyperextending (swinging too far ahead of the upper leg, or thigh) by means of angular stops at the knees. Thus, the kneed walkers have an internal rotational collision. In our modeling, we assume that all collisions are instantaneous and non-bouncing (plastic).

Following McGeer, our analysis is built around simulation of a single walking step. One step, or cycle of motion, starts at an arbitrary point, say just after a foot collision. A cycle then includes the motion between foot collisions, as well as the discontinuities at the next foot collision. The cycle of motion is represented mathematically by a return map, termed the 'stride-function' by McGeer, that maps the state of the system from just after one heel-strike to just after the next. Fixed points of the map correspond to period-one motion cycles, or period-one 'gaits' of the model.

Gait stability can be determined by calculating (most often numerically) the eigenvalues of the linearization of the map at the fixed points (see [3] for a detailed description of the modeling and analysis procedures).

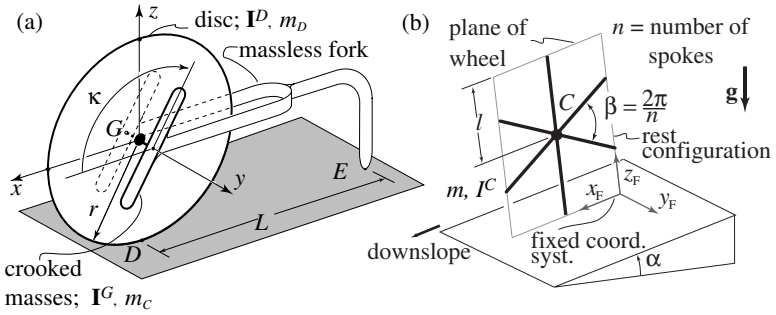

Figure 1. The parameters and orientation variables for (a) a uniform rolling disk with oblique masses added and (b) a rimless spoked wheel.

Using this scheme, we have studied several passive-dynamic models of increasing complexity, progressing from rolling wheels to 2D straight-legged and kneed models to 3D straight-legged models, each of which is described below. We also describe a simple barely-controlled powering scheme for a 2D straight-leg walker, which produces stable gait on level ground.

2. Rolling Wheels in 2D and 3D

Perhaps the simplest passive-dynamic system to study, that has some features in common with walking, is the rimless spoked wheel, or rolling polygon, confined to 2D [8]. The 2D rimless wheel has a stable limit cycle motion whose eigenvalues and associated global basins of attraction we have completely determined analytically [3]. The primary lesson of the rimless wheel in 2D is that speed regulation comes from a balance of collisional dissipation, which is proportional to speed squared, and gravitational work, which is proportional to speed.

Next, we studied a 3D rolling disk with oblique masses added [3] (see Figure 1). The masses can bank and steer with the disk but cannot roll (or pitch) with it. The purpose of this investigation was to study the effects of mass distribution on stability. The oblique masses, if adjusted properly, change the stability of the uniform rolling disk, a conservative nonholonomic system, from neutrally stable to asymptotically stable [10]. This result suggests that mass distribution may affect side-to-side balance in more complicated walking models.

Finally, we studied the 3D rimless wheel (see Figure 1) and found analytically, for many spokes and small slope angles, the stability eigenvalues for steady 'rolling' motions [1]. The 3D rimless wheel is a piecewise-

conservative-holonomic (but globally non-conservative and nonholonomic) system with intermittent, dissipative impacts – features that are shared by some more realistic human walking models. The rolling rimless wheel can also exhibit asymptotic stability when perturbed from a downhill limit cycle, even when its mass distribution corresponds to that of a disk that does nothave asymptotic stability. Thus, the intermittent collisions can play a role in side-to-side balance.

Despite the useful lessons from rolling models, they are not anthropomorphic walkers. They cannot fall down forwards or backwards, and they lack swinging legs.

3. Straight-Legged 2D Walkers

The next-simplest class of models live in 2D and consist of two linked swinging legs and point-feet [8, 6, 3, 5]. Asymptotically-stable walking motions of these models exist for a variety of parameters. The simplest such 'point-foot' straight-legged model has a huge hip mass and tiny masses (relatively infinitesimal) at its point-feet (see Figure 2).

A typical plot of the stance-leg and swing-leg angles is shown over one stable step in Figure 2. This model exhibits two steady walking motions, or period-one gaits, all the way to ! 0^+ as shown in Figure 3. At these gaits, the stance angle (and step length) are proportional to $^{1=3}$. Figure 4 shows how stable limping (period-two) and apparently-chaotic 'staggering' gaits appear as the slope angle is increased.

That this machine can walk on arbitrarily small slopes means that, by some reasonable measures, it is capable of near-perfectly-efficient gait (zero+ energy cost per unit distance of transport). At small slopes, the gravitational power used by this model in downhill walking is proportional to the fourth power of the walking speed. This result gives insight into achieving similar efficiency in more complicated models (e.g. models with knees, circular feet, and/or more general mass distribution). The power scaling depends, in part, on the infinitesimally small feet. With finite-mass feet, there are two modes of energy loss at heelstrike: one due to deflection of the hip mass, and one due to dissipation of the foot's kinetic energy in a plastic collision with the ground. Preliminary studies of point-foot models with finite foot mass show that the long-period gaits retain the same scaling laws at small slopes, while the short-period gaits do not.

4. More General 2D Walkers

We have reproduced and extended McGeer's results for more general 2D walkers with knees[8]: Figure 5 shows the state variables and parameters for

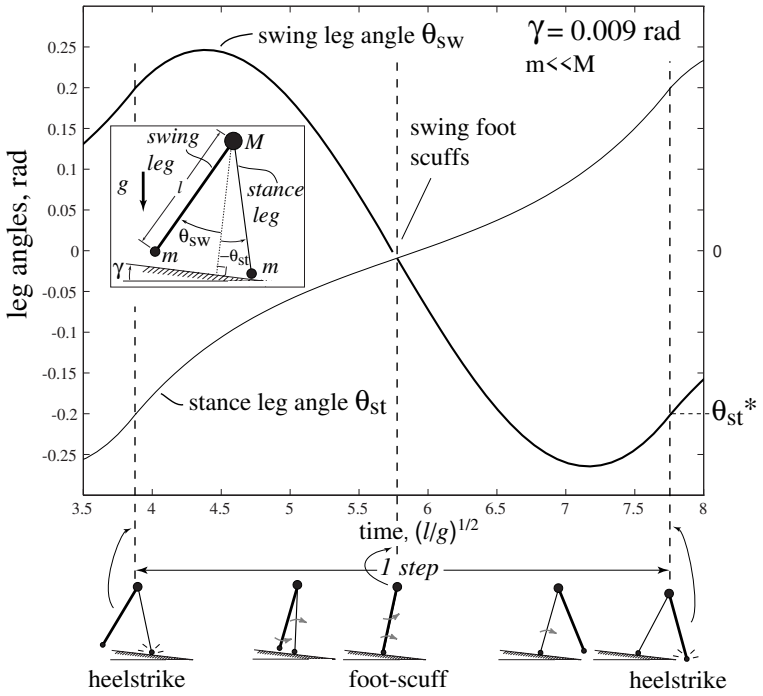

Figure 2. The simplest walking model and one of its typical passive walking steps. The inset schematic describes the variables and parameters that we use. In the cartoon below the graph, the new stance leg (lighter line) has just made contact with the ramp (left-most picture). The swing leg (heavier line) swings until the next heel-strike (right-most picture). We ignore foot-scuffing of the swing leg, allowing its foot to pass through the floor. Leg angles versus time are shown over one step at a gait cycle. Leg lines are drawn with different weights to correspond to heavy-line leg of the cartoon below the graph. Heelstrike returns the system to its initial conditions. A perturbation analysis predicts $_{st}{}' \ldots C_1 \; {}^{1=3} + C_2$, where $_{st}{}'$ is the stance angle at a fixed point (see Garcia, *et al.* [5]).

the kneed model and Figure 6 shows a typical gait cycle and its qualitative comparison to experimental data.

Certain conditions on the mass distribution are necessary for general 2D kneed and straight-legged walkers to achieve walking at arbitrarily small slope angles. These 'balanced' models follow similar scaling laws as their simpler point-foot, straight-legged cousins. We have also found period doubling and chaos for these kneed walkers.

5. 3D Walking

Finally, we move our point-foot model into 3D [3]. McGeer [9] and Fowble and Kuo [4] began studies of three-dimensional passive walking mechanisms, finding only unstable periodic motions. We have built a simple two-

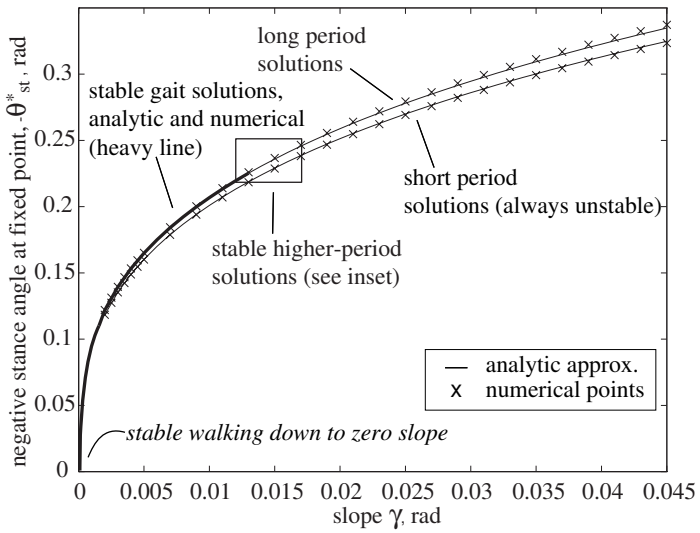

Figure 3. Comparison of numerical and analytic predictions for point-foot stance angle at fixed point as a function of slope. The box is shown expanded in Figure 4.

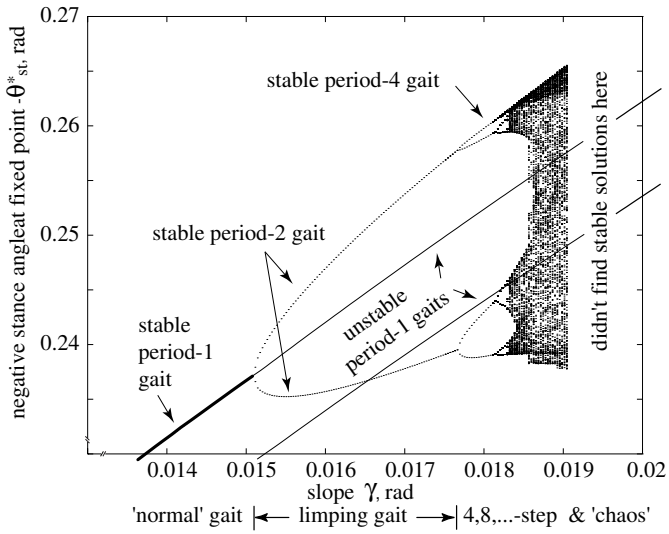

Figure 4. Period doubling of stable walking motions, inset from Figure 3. Period doubling occurs when one of the map eigenvalues for a period-n walking cycle passes through ¡ 1. Unstable period-one cycles are shown for reference. Dotted lines represent stable cycles while solid lines represent unstable ones. No persistent walking was found at slopes much steeper than 0.019 radians.

legged Tinkertoy^{R} model that walks passively, apparently stably, down gentle slopes [2] (see Figure 7).

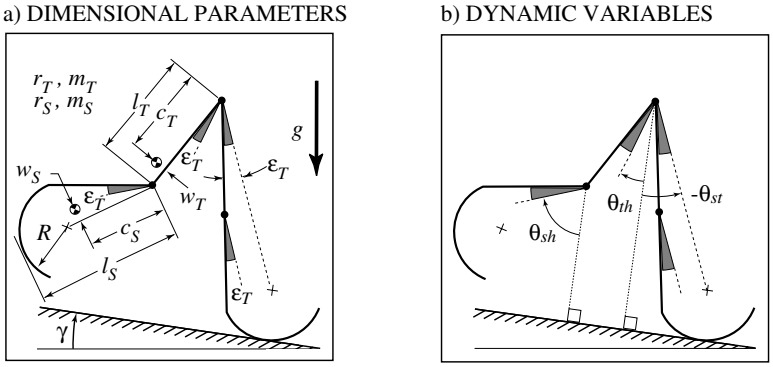

Figure 5. McGeer's kneed walking model. Shown above are (a) model parameters, and (b) dynamic variables. Radii of gyration and masses of thigh and shank are denoted by r_T, m_T, r_S, and m_S, respectively. The foot is a circular arc centered at the "+". γ_T is defined to be the angle between the stance thigh and the line connecting the hip to the foot center. Dynamic variable values θ_{st}, θ_{th}, and θ_{sh} are measured from ground-normal to lines offset by γ_T from their respective segments. A stop (not shown) at each knee prevents hyperextension of either knee.

The configuration and mass distribution of the legs of the Tinkertoy® model were suggested by numerical simulations of a simpler 3D model (see Figure 8) that was predicted to be almost-stable. The model predicts near-stable steady 3D walking solutions (the maximum return map eigenvalue is $|\lambda|_{max} \approx 1.15$ with all others < 1) for very low center-of-mass and lateral center-of-mass location comparable to the leg length. As the lateral center-of-mass position get very large, the model predicts something like 'tight-rope' walking with a long balance bar: the step period and length get very small, and the maximum map eigenvalue modulus approaches 1 (neutral stability) asymptotically from above (see Figure 10). More detailed 3D modeling is currently in progress. This walking mechanism joins a small list of passive mechanical devices free to move in three dimensions but without fast spinning parts, that are statically unstable, yet can be dynamically, asymptotically stable. Figure 9 shows typical 3D periodic behavior predicted by the model.

6. Powered 'Passive' Walking

Once power is added to our passive devices, they are, of course, no longer uncontrolled in the pure sense. Nevertheless, as shown by McGeer [7], a stable passive-dynamic model is a good basis for simple 'open-loop' powering schemes. Figure 11 shows the configuration and simulated walking cycle for a powered 2D point-foot-like model. The torque is provided by a constant-voltage DC motor at the stance-ankle. The ankle is locked during the passive mode.

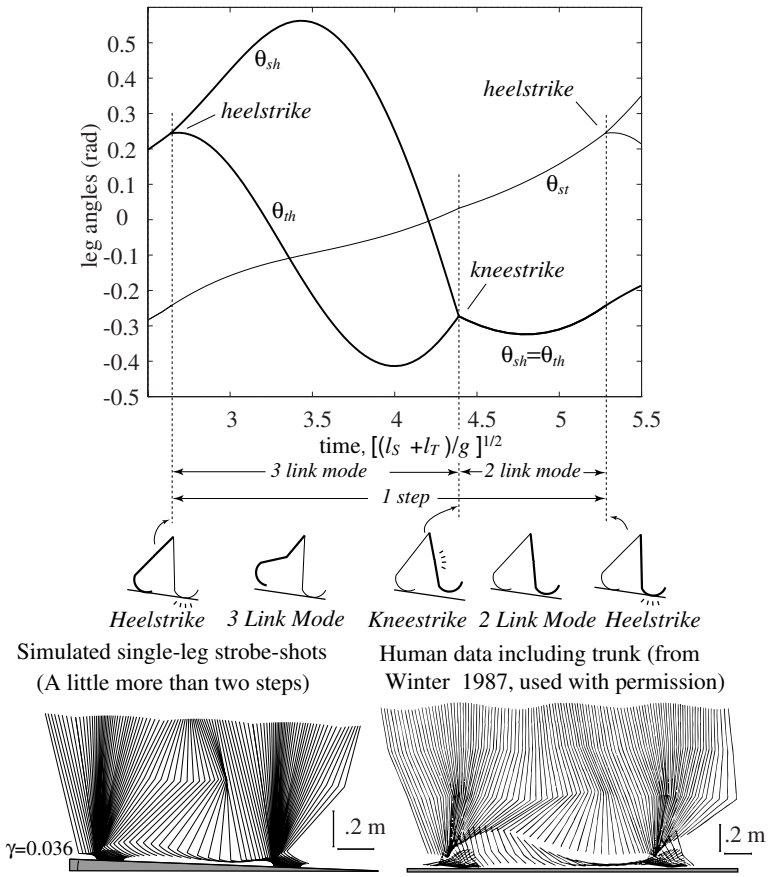

Figure 6. Simulated gait cycle (ours, similar to McGeer's). Angles of leg segments are shown from just before one heelstrike to just after the next heelstrike in a stable gait of the walker in Figure 5. The heavy line on the graph corresponds to the motion of the heavy-line leg on the small cartoon under the graph. At the start of the step, this is the stance leg, but it becomes the swing leg just after the first heelstrike. The strobe-like picture of the walker on the bottom left, created from the simulated gait cycle in the graph, shows the anthropomorphic nature of the gait. The stroboscopic picture on the lower right was generated from experimental data from [11]. The parameters values used, from a working physical model in our lab, are: $l_t = 0.35$m, $w_t = 0$m, $m_t = 2.345$kg, $r_t = 0.099$m, $c_t = 0.091$m, $l_s = 0.46$m, $w_s = 0.025$m, $m_s = 1.013$kg, $r_s = 0.197$m, $c_s = 0.17$m, $R = 0.2$m, $\quad = 0.036$rad, $g = 9.81$ m/s^2, $\gamma_T = 0.097$rad.

7. Conclusions

The human-like and complicated motions of McGeer-like passive dynamic devices studied by ourselves and others imply that coordination in locomotion may be largely governed by pure mechanics. It has yet to be determined whether or not these models have medically-useful lessons to teach us, and whether or not they are a good spring-board for biomechanical or robotic

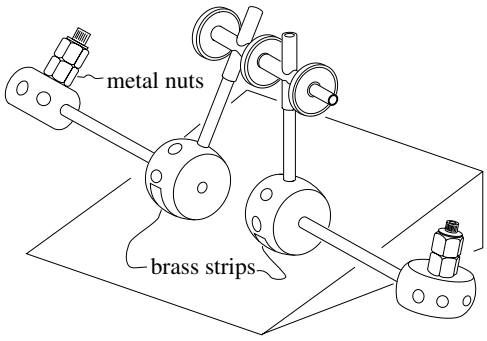

Figure 7. A drawing of our 3D Tinkertoy^{R} walking model. The center-of-mass of the device is above the centers of the wheel-like feet and behind the leg axes. The metal nuts for weight and the brass strips to round the foot bottoms are fastened with black electrical tape.

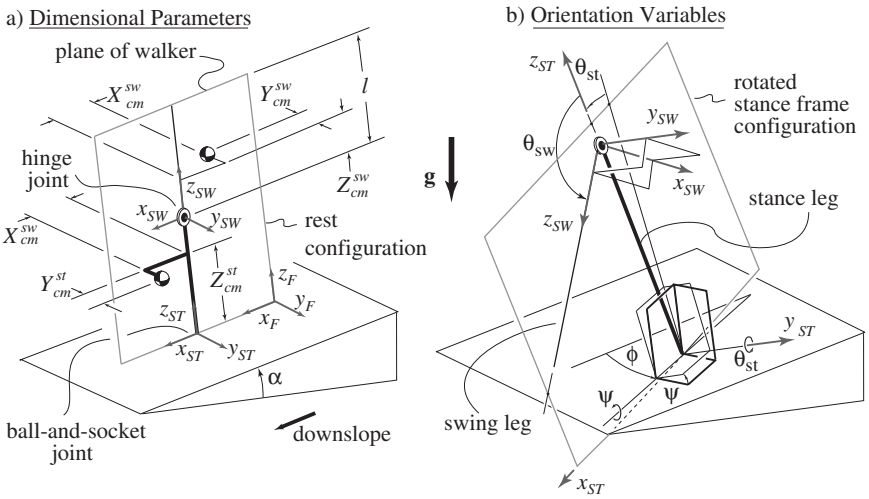

Figure 8. The orientation variables and parameters for the 3D straight-legged point-foot walking model. Each leg has mass `M` , moment of inertia matrix $\mathtt{I}^{\mathtt{cm}}$, and length `l`

models that incorporate neuro-muscular elements or mechanical actuators.

References

1. M. Coleman, A. Chatterjee, and A. Ruina. Motions of a rimless spoked wheel: A simple 3D system with impacts. *Dynamics and Stability of Systems*, 1997. In press.
2. M. Coleman and A. Ruina. A Tinkertoy^{R} model that walks. *Physical Review Letters*, 1997. accepted for publication.
3. M. J. Coleman. *A Stability Study of a Three-dimensional Passive-dynamic Model of Human Gait*. PhD thesis, Cornell University, Ithaca, NY, 1997. In preparation.
4. J. V. Fowble and A. D. Kuo. Stability and control of passive locomotion in 3-D.

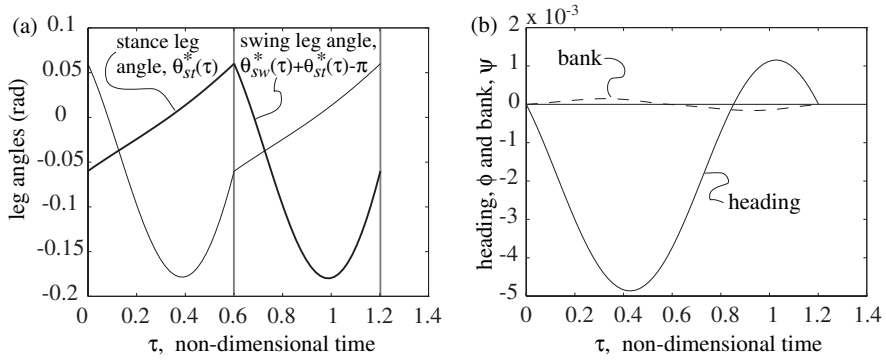

Figure 9. Simple 3-D simulations. Typical periodic gait cycle behavior over two steps for $I_{xx} = 0.5577$, $I_{yy} = 0.0021$, $I_{zz} = 0.5579$, $I_{xy} = 0.0000$, $I_{xz} = 0.0$, $I_{yz} = 0.0$, $fi = 0.0037$, $x = 0.0$, $y = 0.2706$, and $z = 0.9270$. The fixed point for this case is $q^* = [0.0000\ 0.0000\ 0.0008\ -0.0597\ 3.2610\ -0.0132\ 0.0051\ 0.1866\ -0.8523]^T$; the maximum eigenvalue is $|\lambda_{max}| = 2.58$ and the non-dimensional step period is $\tau^* = 1.2031$. (a) The periodic gait cycle leg angles are very similar to those for 2D walking. The heavy line on the graph corresponds to the motion of the heavy-lined leg in Figure 8. At start-of-step, this is the stance leg, but at a foot-collision, it becomes the swing leg. The instants of foot-strike are denoted by the light gray lines. (b) The plots show the relationship of the heading and the bank angle of the walker over two steps.

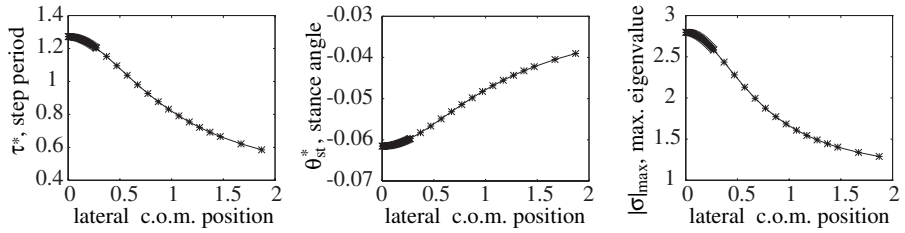

Figure 10. Point-foot 3D simulation. The effect of lateral c.o.m. mass position on the limit cycle period, stance angle, and maximum eigenvalue modulus. Note that the simple simulation does *not* predict stability whereas the more complex physical model *is* stable.

In *Biomechanics and Neural Control of Movement*, pages 28–29, Mount Sterling, Ohio, 1996. Engineering Foundation Conferences.

5. M. Garcia, A. Chatterjee, A. Ruina, and M. J. Coleman. The simplest walking model: Stability, complexity, and scaling. *ASME Journal of Biomechanical Engineering*, 1997. In press.
6. A. Goswami, B. Thuilot, and B. Espiau. Compass-like biped robot, part I: Stability and bifurcation of passive gaits. Rapport de recherche 2996, Unité de recherche INRIA Rhône-Alpes, St. Martin, France, October 1996.
7. T. McGeer. Dynamics and control of bipedal locomotion. *Progress in Robotics and Intelligent Systems*, 1990.
8. T. McGeer. Passive dynamic walking. *The International Journal of Robotics Research*, 9(2):62–82, April 1990.
9. T. McGeer. Passive dynamic catalogue. Technical report, Aurora Flight Sciences Corporation, 1991.
10. J. Papadopolous. personal communication, 1996.

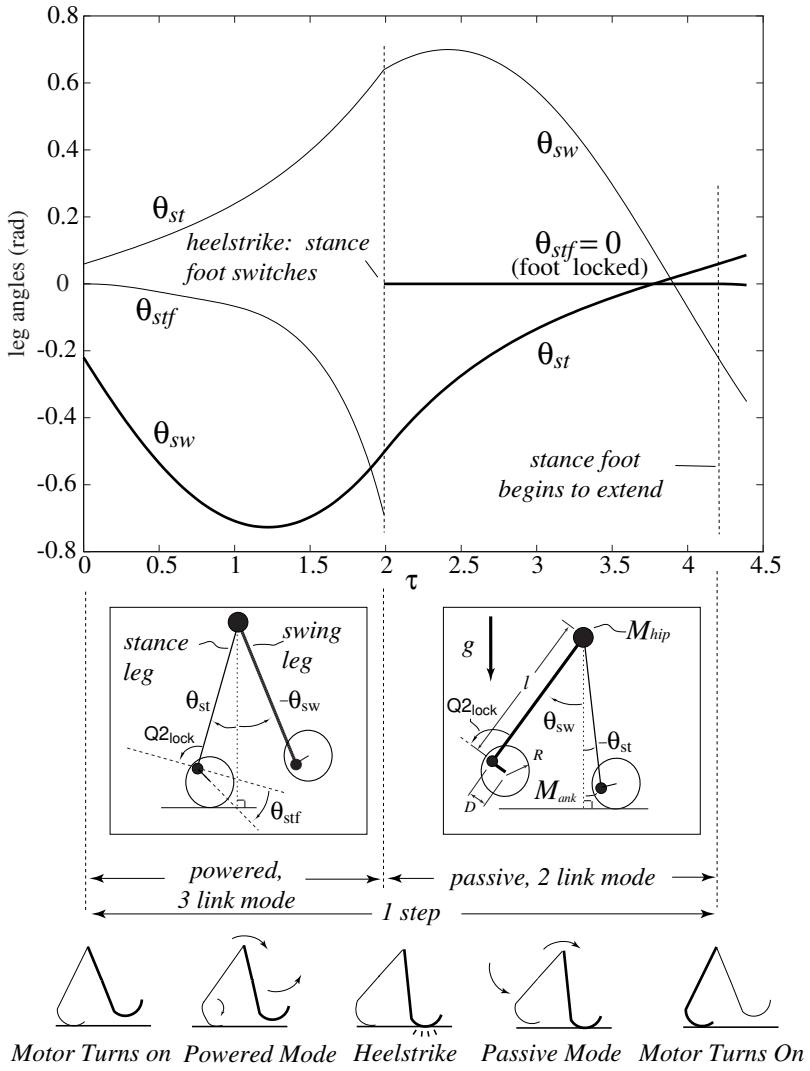

Figure 11. The state of the powered 2D walker versus time over one stable gait cycle. The two inset boxes show the parameters and orientation variables of the 2D powered walker gait cycle. Parameters are as follows: $M_{ank} = 1$; $M_{hip} = 1000$; $l = 1$; $R = 0$; $D = 0.05$; $Q2_{lock} = 3.4$; and $Q3_{switch} = 2.8625$. DC motor characteristics are $\omega_{no\ load} = 100$ and $\tau_{stall} = 725$. The actuation begins when $Q3 = Q3_{switch}$, where $Q3 = \ldots + \theta_{sw} - \theta_{st}$ (the swing leg angle measured from the projection of the stance leg).

11. D. A. Winter. *The Biomechanics and Motor Control of Human Gait.* University of Waterloo Press, Waterloo, Ontario, 1987.